1 **Title: Endocast and bony labyrinth of a stem gnathostome shed light on the earliest**

2 **diversification of jawed vertebrates**

3

4 **Authors:** You-an Zhu[1,2†], Sam Giles[3,4†], Gavin Young[5,6], Yuzhi Hu[5], Mohamad Bazzi[2], Per E.

5 Ahlberg[2], Min Zhu[1,7,8] and Jing Lu[1,7*]

6 **Affiliations:**
7 [1]Key Laboratory of Vertebrate Evolution and Human Origins of Chinese Academy of Sciences,

8 Institute of Vertebrate Paleontology and Paleoanthropology, Chinese Academy of Sciences,

9 Beijing 100044, China.

10 [2]Subdepartment of Evolution and Development, Department of Organismal Biology, Uppsala

11 University, Norbyvägen 18A, SE-752 36 Uppsala, Sweden.

12 [3]School of Geography Earth and Environmental Sciences, University of Birmingham,

13 Birmingham, UK, B15 2TT.

14 [4]Department of Earth Sciences, Natural History Museum, Cromwell Road, London SW7 5BD,

15 UK

16 [5]Department of Applied Mathematics, Research School of Physics, Australian National

17 University, Canberra, ACT, Australia 2601.

18 [6]Australian Museum Research Institute, Sydney, NSW, Australia 2010.

19 [7]CAS Center for Excellence in Life and Paleoenvironment, Beijing 100044, China.

20 [8]University of Chinese Academy of Sciences Beijing 100039, China.

21 [†]These authors contributed equally to this work.

22 *Correspondence to: lujing@ivpp.ac.cn.

23

24 **One Sentence Summary: The skull of a 400-million-year old fossil fish suggests that**
25 **hypotheses of early jawed vertebrate relationships might have to be turned on their**
26 **head.**
27

28 **Abstract:**

29 Our understanding of the earliest evolution of jawed vertebrates depends on a credible

30 phylogenetic assessment of the jawed stem gnathostomes collectively known as 'placoderms'.

31 However, their relationships, and even whether 'placoderms' represent a single radiation or a

32 paraphyletic array, remain contentious. Here we describe the endocranial cavity and inner ear of

33 *Brindabellaspis stensioi*, commonly recovered as a taxon of uncertain affinity branching near the

34 base of 'placoderms'. While some features of its braincase and endocast resemble those of

35 jawless vertebrates, its inner ear displays a repertoire of crown gnathostome characters. Both

36 parsimony and Bayesian analyses suggest that established hypotheses of 'placoderm'

37 relationships are unstable, with newly-revealed anatomy pointing to a potentially radical revision

38 of early gnathostome evolution. Our results call into question the appropriateness of fusiform

39 'placoderms' as models of primitive gnathostome anatomy and raise questions of homology

40 relating to key cranial features.

41 **Main text:** One of the major transitions in vertebrate history was the evolution of gnathostomes,

42 or jawed vertebrates, from jawless ancestors. The major morphological gap apparent when

43 considering only living vertebrate diversity—extant jawless fishes comprise just hagfish and

44 lamprey—is largely filled in by the fossil record (*1*). 'Placoderms', the most crownward

45 assemblage on the gnathostome stem, occupy a pivotal place in this discussion. Traditional

46 hypotheses of relationships posit a monophyletic Placodermi (*2–4*), whereas most recent analyses

47 recover (*2–13*) 'placoderms' as a paraphyletic array from which crown gnathostomes arose (*5–*

48 *11*); but see ref (*12*). In either scenario, taxa recovered near the base of the assemblage are

49 typically dorsoventrally compressed, benthic forms—anatomically similar to agnathan

50 outgroups—with fusiform, nektonic taxa recovered proximate to the gnathostome crown (*1,5,6,8–*

51 *10*); but see ref (*11*). Uncertainty surrounding the relationships between different 'placoderm'

52 groups, as well as their broader taxonomic status, are compounded by an uneven understanding of

53   anatomy across the radiation, particularly of the phylogenetically informative braincase and brain

54   cavity—endocast (see Supplementary Materials).

55   *Brindabellaspis stensioi* (*13*) is a 'placoderm'-grade stem gnathostome from the Early

56   Devonian of New South Wales, Australia. Although almost exclusively recovered among the

57   earliest diverging 'placoderms' (*5,6–8,10–11,14–16*), it has variably been allied with rhenanids

58   (*13*) acanthothoracids (*4*) and antiarchs (*12*), some of which are of dubious monophyly.

59   Comparisons with jawless fishes have frequently been drawn on the basis of gross external and

60   braincase anatomy (*13*) and general proportions of the endocast (*1, 17*). Other distinctive features,

61   such as a large endolymphatic cavity, have been interpreted as autapomorphies (*13, 18*). Here, we

62   provide high-resolution CT data of two more recently discovered specimens (Fig. 1, Fig. S1-4),

63   detailing unexplored parts of the endocast and allowing previously described regions of the

64   braincase and skull roof to be reinterpreted.

65   Tomographic data reveals the position of dermal bone sutures, clarifying the structure of

66   the skull roof. Unlike in previous interpretations (*13,19*), we identify an independent median

67   pineal plate sitting posterior to the rostropineal. We also confirm the presence of four bones

68   contributing to the lateral margin of the skull roof, contra refs (*13,19*). *Brindabellaspis* possesses

69   an elongate ossification (postmarginal) flanking the serial lateral line-bearing bones, resembling

70   maxillate 'placoderms' (*6,10*) and early osteichthyans (*20*); in most other 'placoderms', the

71   postmarginal is either much reduced or lost (*3*).

72   Broadly speaking, our results affirm past descriptions of the endocavity (*13*), although

73   with key clarifications and additions. The extremely short telencephalic region of the endocast

74   has a flat anterior face with no bulge anterior to the olfactory and terminal nerves, contra ref (*13*)

75   (Fig. 1c and e). CT data also clarify that, as in crown gnathostomes (*8,21,22*), the ventral sides of

76   the telencephalic and diencephalic cavities are smooth and continuous between the optic nerve

77   and hypophysis, rather than displaying a step-like transition as in most 'placoderms' (*18,23*) (Fig.

78   S5). We also confirm that the hypophysis is oriented anteriorly (*13*) (Fig. 1e). Although an

79   anteriorly (or ventrally) directed hypophysis has sometimes been considered restricted to

80   agnathans and 'placoderms'(*18*), it is also reported in crown gnathostomes (*16,22,24*). Characters

81   previously suggested as being shared between agnathans and *Brindabellaspis*, such as a laterally

82   expansive cerebellum and anteroposteriorly elongate vagus complex (Fig. 1d and f, Fig. S3), are

83   now known to be widespread in other stem and crown gnathostomes (*16,18,22*) (Fig. 2 and Fig.

84   S5), and are presumably plesiomorphic for the gnathostome crown. As described by Young (13),

85   the olfactory tracts are elongate, and diverge anteriorly towards the widely separated and laterally

86   positioned nasal capsules (Fig. 1c and Fig. 2, Fig. S3a-d). Divergent olfactory tracts are otherwise

87   only known in crown gnathostomes (*16,21,22*) in other 'placoderms' and the galeaspid *Shuyu* (*25*)

88   the olfactory tracts are parallel and typically short (Fig. 2). The myelencephalic region of the

89   endocast anterior to the vagus nerve, which is usually proportionately long in most 'placoderms'

90   (Fig. 2 and Fig. S5d-g) but short in agnathans and crown gnathostomes (Fig. 2 and Fig. S5a-c, h-

91   m), appears intermediate in length in *Brindabellaspis*.

92   Our CT data reveal important new anatomical details of the bony labyrinth and

93   endolymphatic complex. In addition to features identified in the endocast, the bony labyrinth of

94   *Brindabellaspis* (Fig. 1c-f, Fig. 2, Fig. S4) bears unexpected similarities to those of crown

95   gnathostomes, with considerable difference to those of other 'placoderms'. The labyrinth is

96   anteroposteriorly short, and all three semicircular canals have large diameters. The anterior

97   semicircular canal is significantly shorter than its posterior counterpart, and in dorsal view the

98   two diverge at a much smaller angle than in other 'placoderms' such as the rhenanid *Jagorina*

99   and arthrodire *Kujdanowiaspis* (Figs. 1c-f and 3, Fig. S4). Most strikingly, CT data demonstrate

100   that the anterior and posterior semicircular canals of *Brindabellaspis* join in a crus commune,

101   with a pronounced sinus superior developed ventrally. This configuration is typical of crown

102   gnathostomes (*16,21,22*), and the combination is unknown in other 'placoderms' (Fig. 3). There

103   is no significant preampullary portion of the posterior semicircular canal, and the utriculus does

4

104   not separate the anterior and external semicircular canals (both contra the condition in all known

105   'placoderms' except *Romundina* (*18*)). While incomplete ventrally, the curvature of the sacculus

106   suggests that it is significantly smaller than in other 'placoderms', barely protruding laterally (Fig.

107   2 and Fig. 3). It is also restricted ventral to the plane of the external semicircular canal, a

108   condition seen elsewhere only in crown gnathostomes (Fig. 2 and Fig. 3). Despite the lack of an

109   external semicircular canal or utricular chamber in agnathans (*25*), a number of labyrinth

110   characters can be polarised across the jawless-jawed vertebrate transition. Osteostracans possess

111   small angles between anterior and posterior semicircular canals, and a crus commune but no

112   developed sinus superior (Fig. 3).

113   Although previously considered autapomorphic (*13*), our data allow similarities to be drawn

114   between the endolymphatic systems of *Brindabellaspis* and crown gnathostomes. The complex in

115   *Brindabellaspis* can be divided into three distinct sections: a large, well-developed endolymphatic

116   sac; an ascending duct connecting the vestibular chamber to the endolymphatic sac; and a distal

117   duct extending from the sac, through the dermal bone, and opening externally (Figs. 1d-f, Fig. 2

118   and Fig. 3, Fig. S4a, d-f). There is no "second sac", contra ref (*18*). In both jawless and jawed

119   stem gnathostomes, the endolymphatic complex is a simple tube-like structure that extends

120   unidirectionally, and is positioned close to the labyrinth (*17,18,23,25*). In contrast, the crown

121   gnathostome system is more complex and divided into three distinct regions (*26*), much as in

122   *Brindabellaspis*, and located mesially, closer to the brain cavity than the labyrinth (*27,28*) (Fig. 2

123   and Fig. 3).

124   A revised and expanded morphological matrix, analysed under both parsimony and Bayesian

125   frameworks, provides novel—and conflicting—insights into early gnathostome evolution. Under

126   parsimony analysis, jaw-bearing gnathostomes fall into one of two monophyletic groups (Fig. 3

127   and Fig. S7a). The more stemward of these contains the bulk of traditionally-recognised

128   'placoderms', albeit with arthodires representing a nested radiation within this clade.

129   Unexpectedly, *Brindabellaspis* is recovered as the earliest diverging member of a clade

130   comprising, successively: antiarchs, maxillate 'placoderms', and crown gnathostomes. The

131   position of antiarchs as proximate to the gnathostome crown, with arthrodires representing an

132   independently fusiform radiation, is unexpected (*1,5,6,8–10*); but see ref (*12*), and perhaps

133   indicates the importance of endocranial data and previous biases towards external morphology.

134   The endocavities of *Minicrania* (*29*) and *Phymolepis* (*30*) hint at the presence of a mesially-

135   directed endolymphatic duct and an endolymphatic sac, as well as a relatively short hindbrain.

136   Although not included in the phylogenetic analysis, these anatomical similarities between the

137   endocrania of antiarchs and *Brindabellaspis*—and, by extension, the gnathostome crown—lend

138   support to the hypothesis of relationships suggested in our parsimony results. However, support

139   values amongst early gnathostomes are low, and the proximity of antiarchs to the gnathostome

140   crown node raises several questions of homology. The transition from posteriorly-positioned to

141   anteriorly-positioned nasal capsules, as well as changes to jaw suspension, are now optimised as

142   evolving twice: once within the clade comprising *Romundina*, rhenanids, ptyctodonts,

143   petalichthyids and arthrodires; and once within the clade comprising maxillate 'placoderms' and

144   crown gnathostomes. The recovery of arthrodires as removed from maxillate 'placoderms' plus

145   crown gnathostomes also requires a number of homoplasies in the skull roof and trunk armour.

146   Results under Bayesian analyses differ from our parsimony analysis and recall more

147   common hypotheses of placoderm paraphyly (*1,5,6,8–10*), with antiarchs recovered as the

148   earliest-diverging 'placoderm' clade and arthrodires as sister taxa to maxillate 'placoderms' and

149   the gnathostome crown. Outside of these nodes, however, other 'placoderms'—including

150   *Brindabellaspis*—fall in a polytomy, and arthrodires are recovered as paraphyletic. Resolving this

151   conflict represents a fundamental challenge of early gnathostome evolution, and is one that

152   cannot be resolved without detailed CT-based reassessment of the anatomy of key 'placoderm'

153   taxa.

6

154   Our work adds considerably to knowledge of labyrinth and endocast variation across stem

155   gnathostomes, highlighting the major impact that CT-based descriptions and re-examination of

156   key taxa can have on both phylogenetic resolution and schemes of morphological evolution. The

157   unexpected character combination in *Brindabellaspis* suggests that endocranial characters

158   previously considered exclusive to crown gnathostome are likely widely distributed amongst a

159   diversity of stem jawed vertebrates. However, outstanding questions remain about the homology

160   of features common to both arthrodires and crown gnathostomes, notably in the skull roof and

161   nasal capsules. The conflicting phylogenetic hypotheses of relationships presented here highlight

162   major uncertainties on the gnathostome stem, calling into question long-standing assumptions

163   about patterns of character evolution. Recent work on the diversity of 'acanthothoracid'

164   dentitions, also revealed by CT data, suggests a more complex picture of dental character

165   evolution and provides independent evidence that at least some 'acanthothoracids' may branch

166   closer to the gnathostome crown node than previously thought (*11*). Notably, the position of

167   arthrodires as removed from maxillate 'placoderms' plus crown gnathostomes challenges

168   previous installations of fusiform, arthrodire-like taxa as a representative of the primitive

169   gnathostome condition (*10,23,31*).

170

171   **References and Notes:**

172   1. P. Janvier, *Early Vertebrates* (Clarendon Press; Oxford University Press, Oxford, 1996)

173   2. G. C. Young, The relationships of placoderm fishes. *Zool. J. Linn. Soc.* **88**, 1–57 (1986).

174   3. G. C. Young, Placoderms (armored fish): dominant vertebrates of the Devonian period.

175   *Annu. Rev. Earth Planet. Sci.* **38**, 523–550 (2010).

176   4. D. Goujet, G. C. Young. in *Recent Advances in the Origin and Early Radiation of*

177   *Vertebrates* (eds G. Arratia, M. V. H. Wilson, & R. Cloutier) 109–126 (Verlag Dr.

178   Friedrich Pfeil, 2004).

179   5. M. D. Brazeau, The braincase and jaws of a Devonian 'acanthodian' and modern

180   gnathostome origins. *Nature* **457**, 305–308 (2009).

181   6. M. Zhu, X. Yu, P. E. Ahlberg, B. Choo, J. Lu, T. Qiao, Q. Qu, W. Zhao, L. Jia, H. Blom,

182   Y. Zhu, A Silurian placoderm with osteichthyan-like marginal jaw bones. *Nature* **502**,

183   188–193 (2013).

184   7. M. D. Brazeau, M. Friedman, The origin and early phylogenetic history of jawed

185   vertebrates. *Nature* **520**, 490–497 (2015).

186   8. S. Giles, M. Friedman, M. D. Brazeau, Osteichthyan-like cranial conditions in an Early

187   Devonian stem gnathostome. *Nature* **520**, 82–85 (2015).

188   9. J. A. Long, E. Mark-Kurik, Z. Johanson, M. S. Y. Lee, G. C. Young, Z. Min, P. E.

189   Ahlberg, M. Newman, R. Jones, J. den Blaauwen, B. Choo, K. Trinajstic, Copulation in

190   antiarch placoderms and the origin of gnathostome internal fertilization. *Nature* **517**,

191   196–199 (2015).

192   10. Zhu, M. *et al.* A Silurian maxillate placoderm illuminates jaw evolution. *Science* **354**,

193   334–336 (2016).

194   11. V. Vaškaninová, D. Chen, P. Tafforeau, Z. Johanson, B. Ekrt, H. Blom, P. E. Ahlberg,

195   Marginal dentition and multiple dermal jawbones as the ancestral condition of jawed

196   vertebrates. *Science* **369**, 211–216 (2020).

197   12. B. King, T. Qiao, M. S. Y. Lee, M. Zhu, J. A. Long, Bayesian morphological clock

198   methods resurrect placoderm monophyly and reveal rapid early evolution in jawed

199   vertebrates. *Syst. Biol.* **66**, 599–516 (2016).

200   13. G. C. Young, A new Early Devonian placoderm from New South Wales, Australia, with

201   a discussion of placoderm phylogeny. *Palaeontogr. Abt. A* **167**, 10–76 (1980).

202   14. S. P. Davis, J. A. Finarelli, M. I. Coates, *Acanthodes* and shark-like conditions in the last

203   common ancestor of modern gnathostomes. *Nature* **486**, 247–250 (2012).

204 15. T. Qiao, B. King, J. A. Long, P. E. Ahlberg, M. Zhu, Early gnathostome phylogeny

205   revisited: multiple method consensus. *PLoS One* **11**, e0163157 (2016).

206 16. A. M. Clement, B. King, S. Giles, B. Choo, P. E. Ahlberg, G. C. Young, J. A. Long,

207   Neurocranial anatomy of an enigmatic Early Devonian fish sheds light on early

208   osteichthyan evolution. *eLife*. **7**, e34349 (2018).

209 17. P. Janvier, The relationships of the Osteostraci and Galeaspida. *J. Vertebr. Paleontol.***4**,

210   344–358 (1984).

211 18. V. Dupret, S. Sanchez, D. Goujet, P. E. Ahlberg, The internal cranial anatomy of

212   *Romundina stellina* Orvig, 1975 (Vertebrata, Placodermi, Acanthothoraci) and the origin

213   of jawed vertebrates-Anatomical atlas of a primitive gnathostome. *PLoS One* **12**,

214   e0171241 (2017).

215 19. B. King, G. C. Young, J. A. Long, New information on *Brindabellaspis stensioi* Young,

216   1980, highlights morphological disparity in Early Devonian placoderms. *R. Soc. Open Sci.*

217   **5**, 180094 (2018).

218 20. M. Zhu, W. Zhao, L. Jia, J. Lu, T. Qiao, Q. Qu, The oldest articulated osteichthyan

219   reveals mosaic gnathostome characters. *Nature*. **458**, 469–474 (2009).

220 21. J. G. Maisey, Braincase of the Upper Devonian shark *Cladodoides wildungensis*

221   (Chondrichthyes, Elasmobranchii), with observations on the braincase in early

222   chondrichthyans. *Bull. Am. Mus. Nat. Hist.* **288**, (2005).

223 22. S. Giles, M. Friedman, Virtual reconstruction of endocast anatomy in early ray-finned
224   fishes (Osteichthyes, Actinopterygii), *J. Paleontol.* **88**, 636–651 (2014).

225 23. E. A. Stensiö, Anatomical studies on the arthrodiran head. Part 1. Preface, geological and

226   geographical distribution, the organization of the head in the Dolichothoraci,

227   Coccosteomorphi and Pachyosteomorphi. Taxonomic appendix. *Kgl. Svenska.*

228   *Vetenskapsakad. Handl.* **9**, 1–419 (1963).

229 24. M. I. Coates, Endocranial preservation of a Carboniferous actinopterygian from

230   Lancashire, U.K., and the interrelationships of primitive actinopterygians. *Philos. Trans.*

231   *R. Soc. Lond. B. Biol. Sci.* **354**, 435–462 (1999).

232 25. Z. Gai, P. C. J. Donoghue, M. Zhu, P. Janvier, M. Stampanoni, Fossil jawless fish from

233   China foreshadows early jawed vertebrate anatomy. *Nature* **476**, 324–327 (2011).

234 26. Jayne M. Gardiner, Robert E. Hueter, Karen P. Maruska, Joseph A. Sisneros, Brandon M.

235   Casper, David A. Mann, Leo S. Demski, Sensory physiology and behavior of

236   elasmobranchs, in *Biology Of Sharks And Their Relatives* 325–368 (CRC Press, 2004).

237 27. M. I. Coates, R. W. Gess, J. A. Finarelli, K. E. Criswell, K. Tietjen, A symmoriiform

238   chondrichthyan braincase and the origin of chimaeroid fishes. *Nature* **541**, 208–211

239   (2017).

240 28. J. Lu, S. Giles, M. Friedman, M. Zhu, A new stem sarcopterygian illuminates patterns of

241   character evolution in early bony fishes. *Nat. Commun.* **8**, 1932 (2017).

242 29. M. Zhu, P. Janvier, A small antiarch, *Minicrania lirouyii* gen. et sp. nov., from the Early

243   Devonian of Qujing, Yunnan (China), with remarks on antiarch phylogeny. *J. Vert.*

244   *Paleont.* **16**, 1–15 (1996).

245 30. Y. Wang, M. Zhu, Redescription of *Phymolepis cuifengshanensis* (Antiarcha:

246   Yunnanolepididae) using high-resolution computed tomography and new insights into

247   anatomical details of the endocranium in antiarchs. *PeerJ* **6**, e4808 (2018).

248 31. M. Rücklin, P. C. J. Donoghue, Z. Johanson, K. Trinajstic, F. Marone, M. Stampanoni,

249   Development of teeth and jaws in the earliest jawed vertebrates. *Nature* **491**, 748–751

250   (2012).

251

10

264   **Data availability:** The CT data that support the findings of this study, as well as 3D surface files

265   of described material, are shared privately in figshare for review:

266   https://figshare.com/s/d040d38b2e0ae3501f65. All other data files are included in the

267   Supplementary Materials.

268   **Supplementary Materials:**

269   *Materials and Methods*
270   *Supplementary Text*
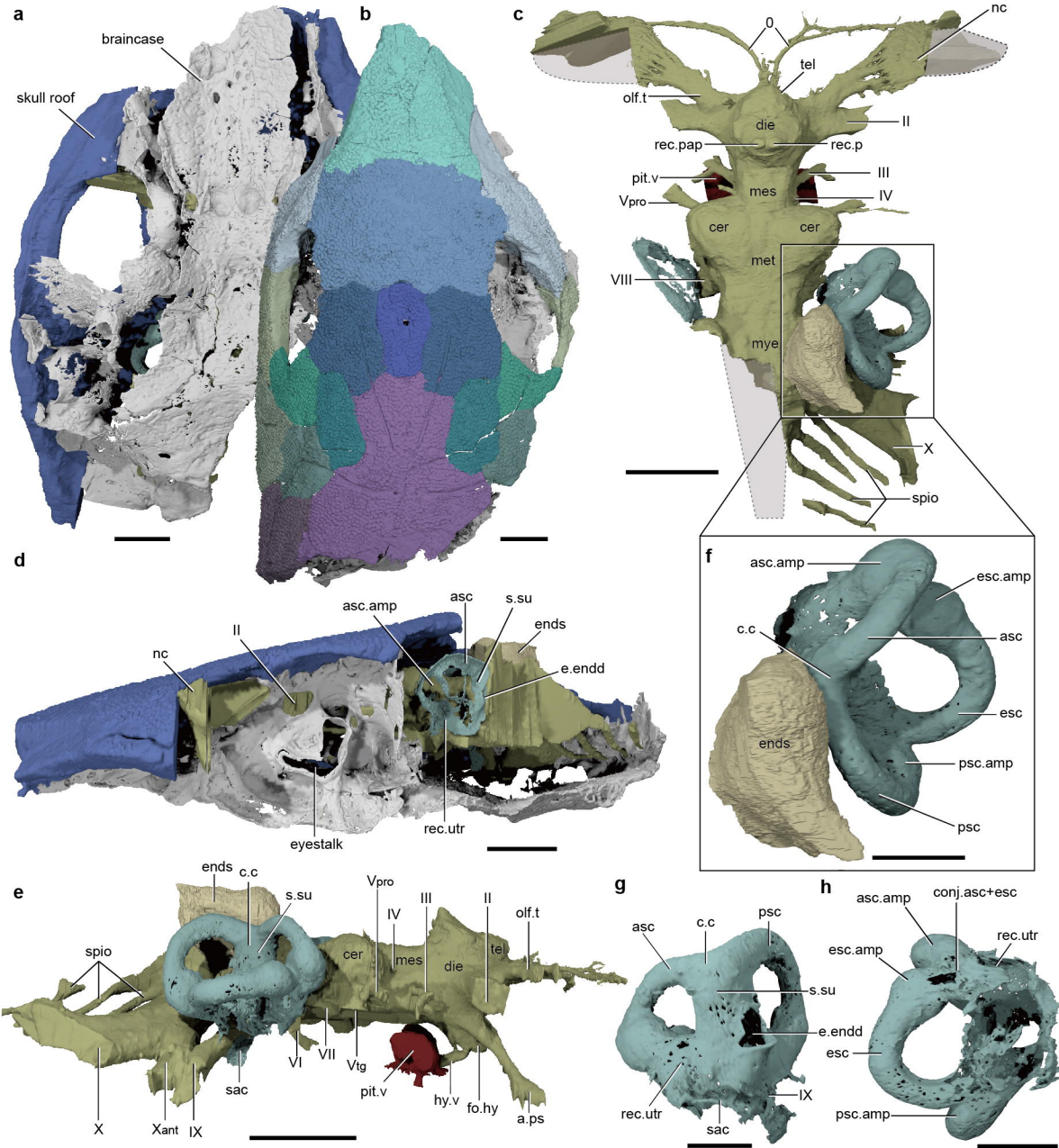271   *Figures S1-S6*
272   *Captions for Data S1 to S5*
273

274   **Figure legends:**

275   **Fig. 1** The skull of the 'placoderm' *Brindabellaspis stensioi*, based on high-resolution CT. **a,**

276   Ventral view of endocranium (ANU 49493). **b**, Dorsal view of skull roof (AM F81911). **c,** Dorsal

277   view of endocranial cavity (ANU 49493,); inset (**f**) shows bony labyrinth and endolymphatic sac

278   region. **d**, Left lateral view of endocranium (ANU 49493). **e**, Right lateral view of endocranial

279   cavity (ANU 49493). **g** and **h**, Mesial and ventral views of the skeletal labyrinth (ANU 49493).

280   Abbreviations: a.ps, efferent pseudobranchial artery; asc, anterior semicircular canal; asc.amp,
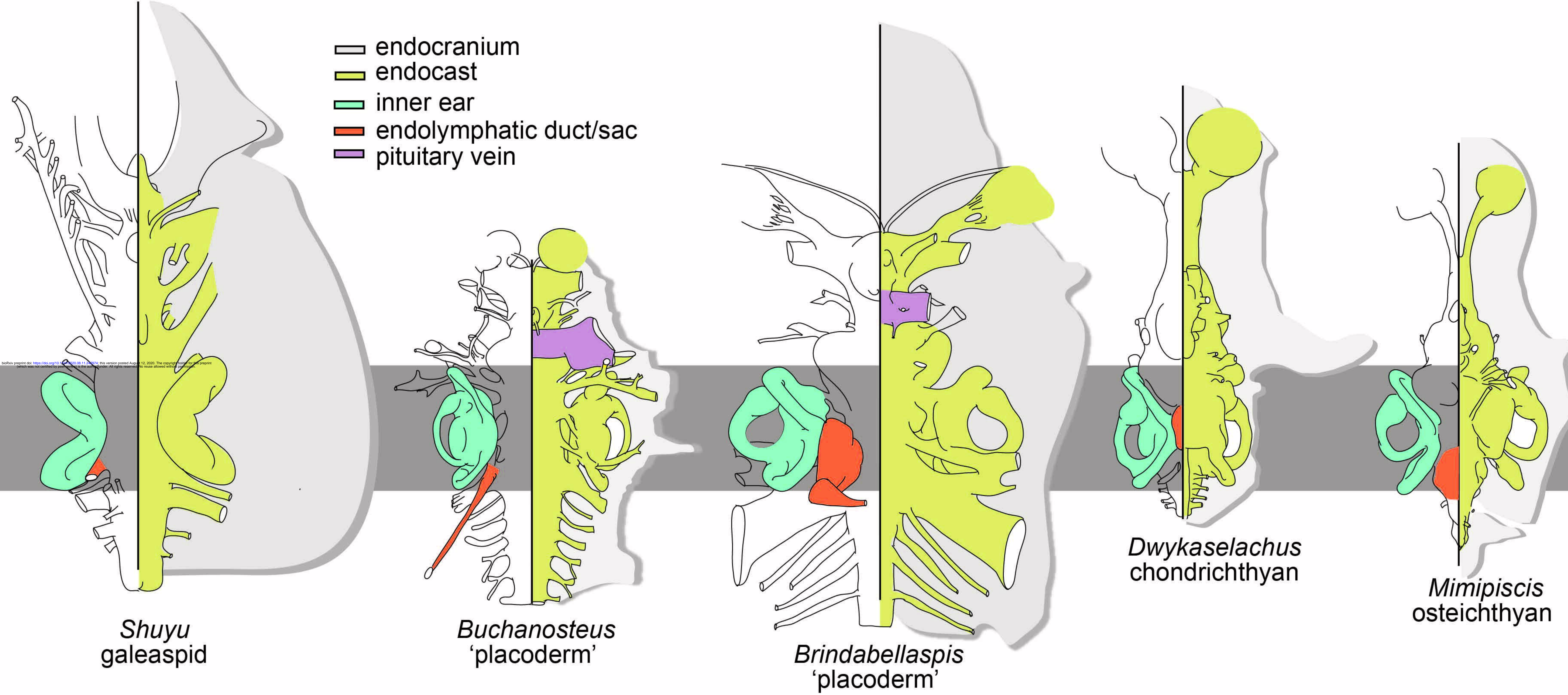
281   ampullae of anterior semicircular canal; c.c, crus commune; conj.asc+esc, conjunction of anterior

282   and external semicircular canals; die, diencephalon; e.endd, exit of endolymphatic duct; ends,

283   endolymphatic sac; esc, external semicircular canal; esc.amp, ampullae of external semicircular

284   canal; fo.hy, hypophysial fossa; hy.v, hypophysial vein; mes, mesencephalon; met,

285   metencephalon; mye, myelencephalon; nc, nasal capsule; olf.t, olfactory tract; pit.v, pituitary vein;

286   psc, posterior semicircular canal; psc.amp, ampullae of posterior semicircular canal; rec.p, pineal

287   recess; rec.pap, parapineal recess; rec.utr, utricular recess; sac, sacculus; spio, spino-occipital

288   nerves; s.su, sinus superior; tel, telencephalon; 0, terminal nerve; II, optic nerve, III, oculomotor

289   nerve; IV, trochlear nerves; Vpro, profundus branch of trigeminal nerve; Vtg, maxillary and

290   mandibular branches of trigeminal nerve; VI, abducens nerve; VII, facial nerve; VIII, otic nerve;

291   IX, glossopharyngeal nerve; X, vagus nerve; Xa, anterior branch of vagus nerve. Scale bars, **a-e**,

292   1 cm; **f-h**, 5 mm.

293   **Fig. 2** Comparative morphology of crania in selected early vertebrates, aligned and scaled to

294   match skeletal labyrinth dimensions (grey bar). Cranial outlines (light grey) and endocast outlines

295   (yellow) in dorsal (left) and ventral (right) views. Data sources for each genus are provided in

296   Supplementary Information.

297   **Fig. 3** Summary phylogeny showing the evolution of the inner ear and endolymphatic complex in

298   early vertebrates. **a,** Simplified phylogeny from the parsimony strict consensus tree (Fig. S6a). **b,**

299   The endolymphatic complex of *Brindabellaspis* and selected crown gnathostomes in lateral view,

300   showing the shared characters including an ascending duct and an endolymphatic sac.
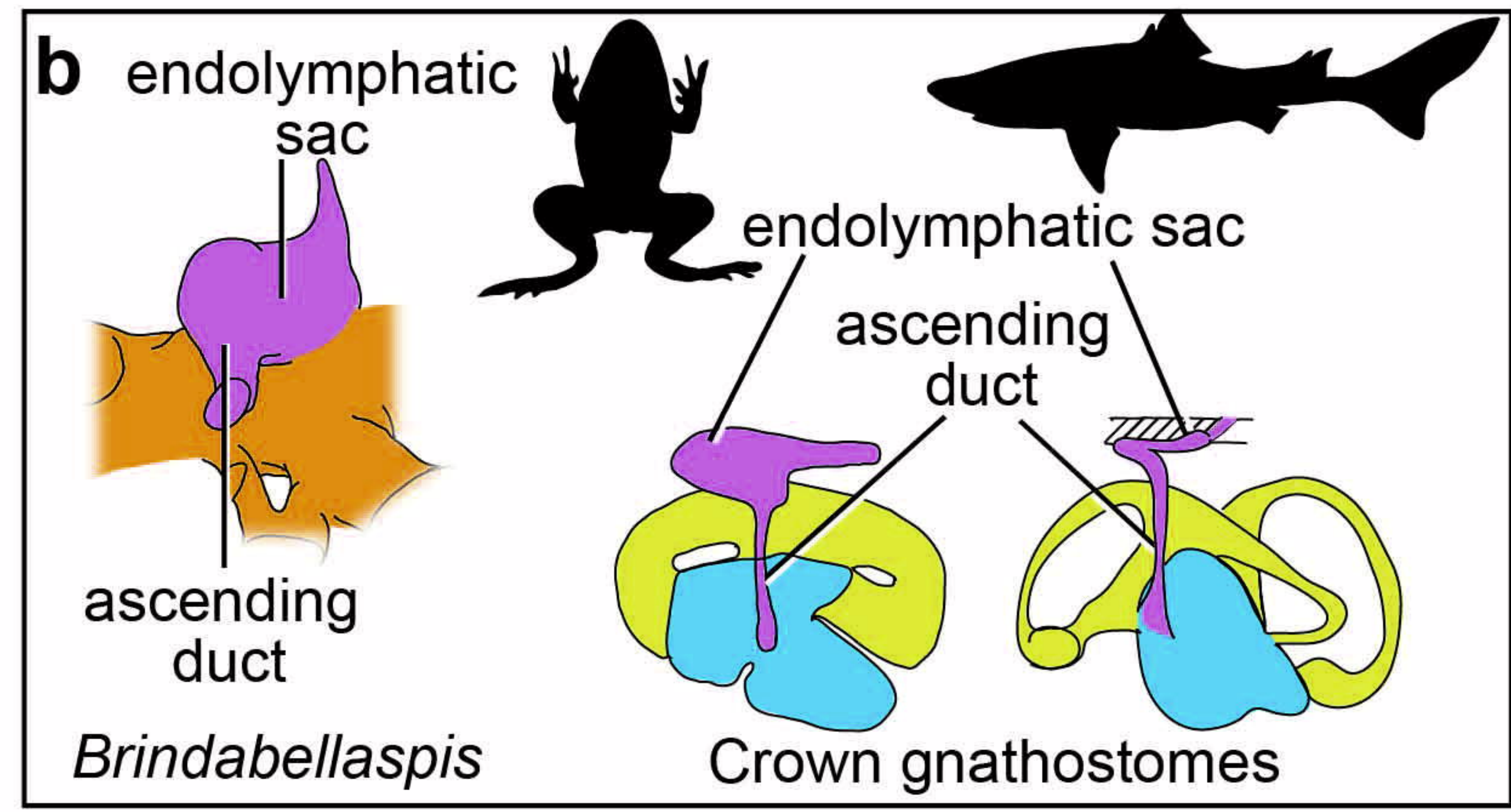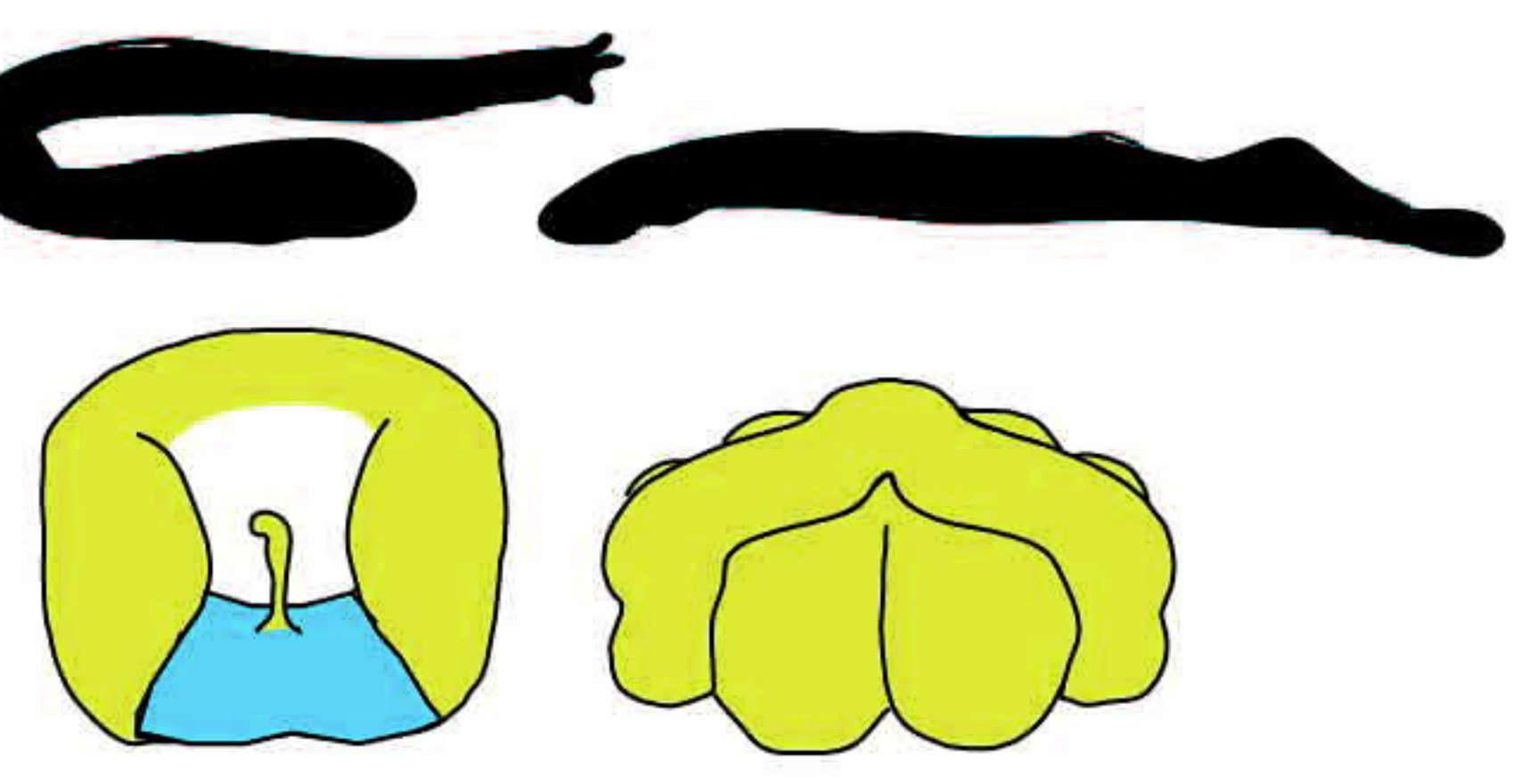
12

endocranium
endocast
inner ear
endolymphatic duct/sac
pituitary vein

Shuyu
galeaspid

Buchanosteus
'placoderm'

Brindabellaspis
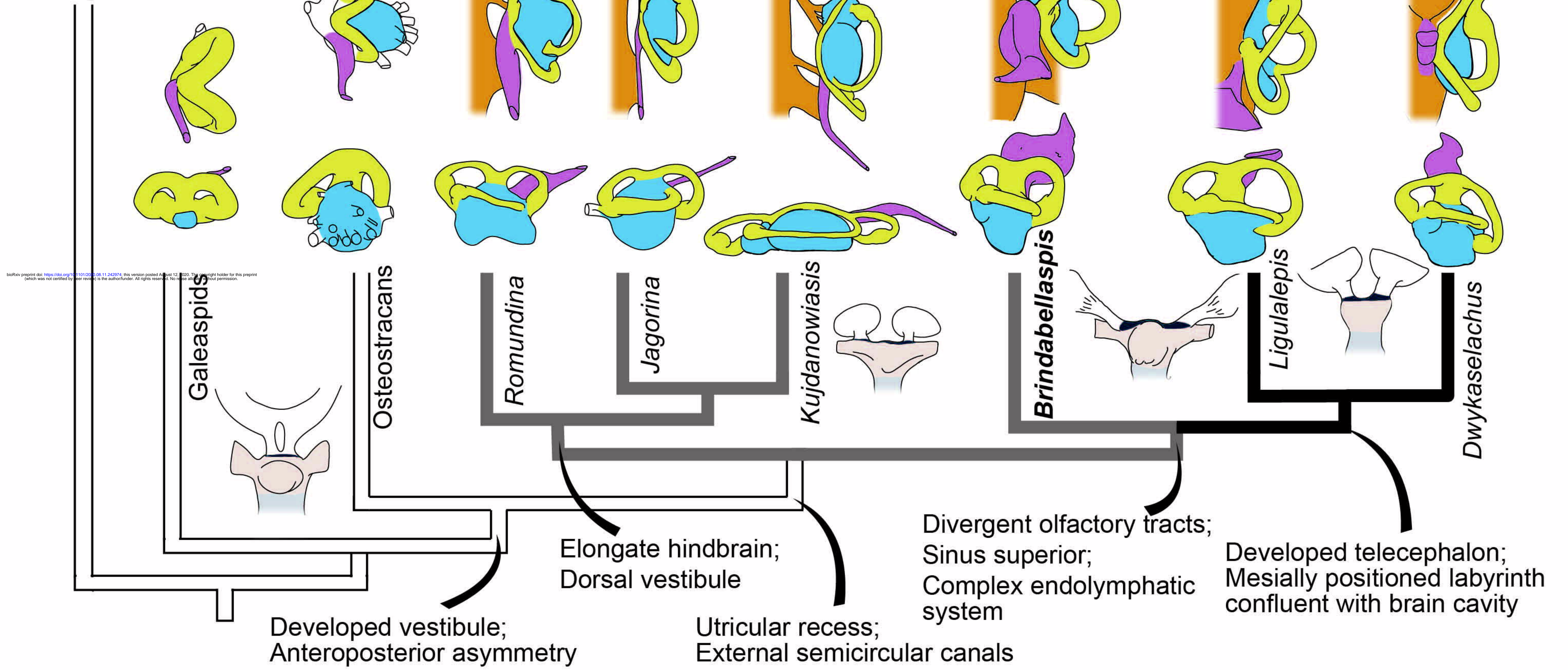'placoderm'

Dwykaselachus
chondrichthyan

Mimipiscis
osteichthyan

a

Jawless fishes
'Placoderms'
Crown gnathostomes

endocast
bony labyrinth
vestibule
endolymphatic complex
nasal capsule / olfactory tracts

telencephalon
diencephalon
mesencephalon

Living agnathans

Galeaspids

Osteostracans

Romundina

Jagorina

Kujdanowiasis

Brindabellaspis

Ligulalepis

Dwykaselachus

Developed vestibule;
Anteroposterior asymmetry

Elongate hindbrain;
Dorsal vestibule

Utricular recess;
External semicircular canals

Divergent olfactory tracts;
Sinus superior;
Complex endolymphatic
system

Developed telecephalon;
Mesially positioned labyrinth
confluent with brain cavity

b

endolymphatic
sac

endolymphatic sac

ascending
duct

ascending
duct

ascending
duct

Brindabellaspis

Crown gnathostomes